



THE NATURE OF TURBULENCE IN SPACE PLASMAS

# *HelioSwarm: Relative Orbit Maintenance in Eccentric P/2 Lunar Resonant Orbit*

Paul Levinson-Muth, Laura Plice, Jose Alvarellos  
Spaceflight Division  
NASA Ames Research Center

2021 AAS/AIAA Astrodynamics Specialist Conference  
Virtual, 9-12 August 2021



University of  
New Hampshire



**NORTHROP GRUMMAN**



Imperial College  
London

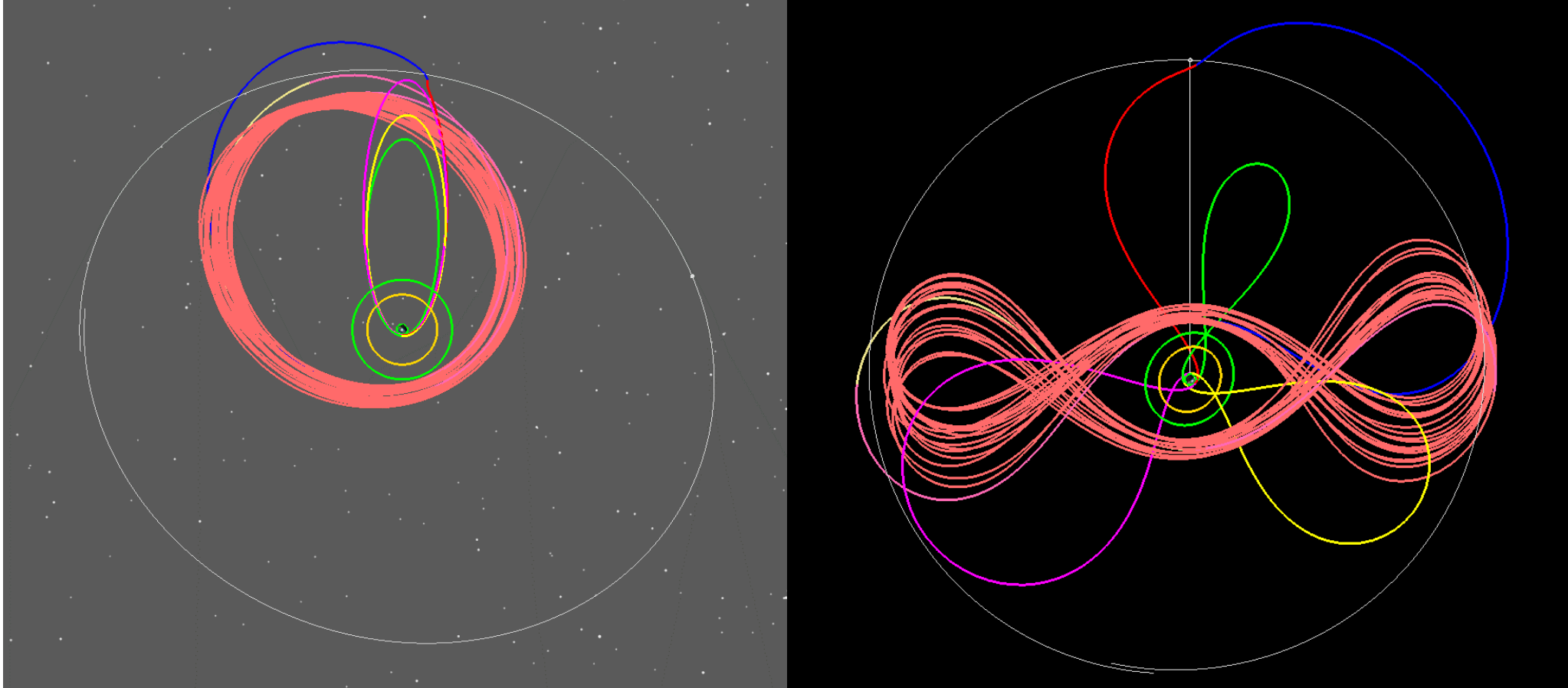
*Goddard*  
Space Flight Center

# Outline



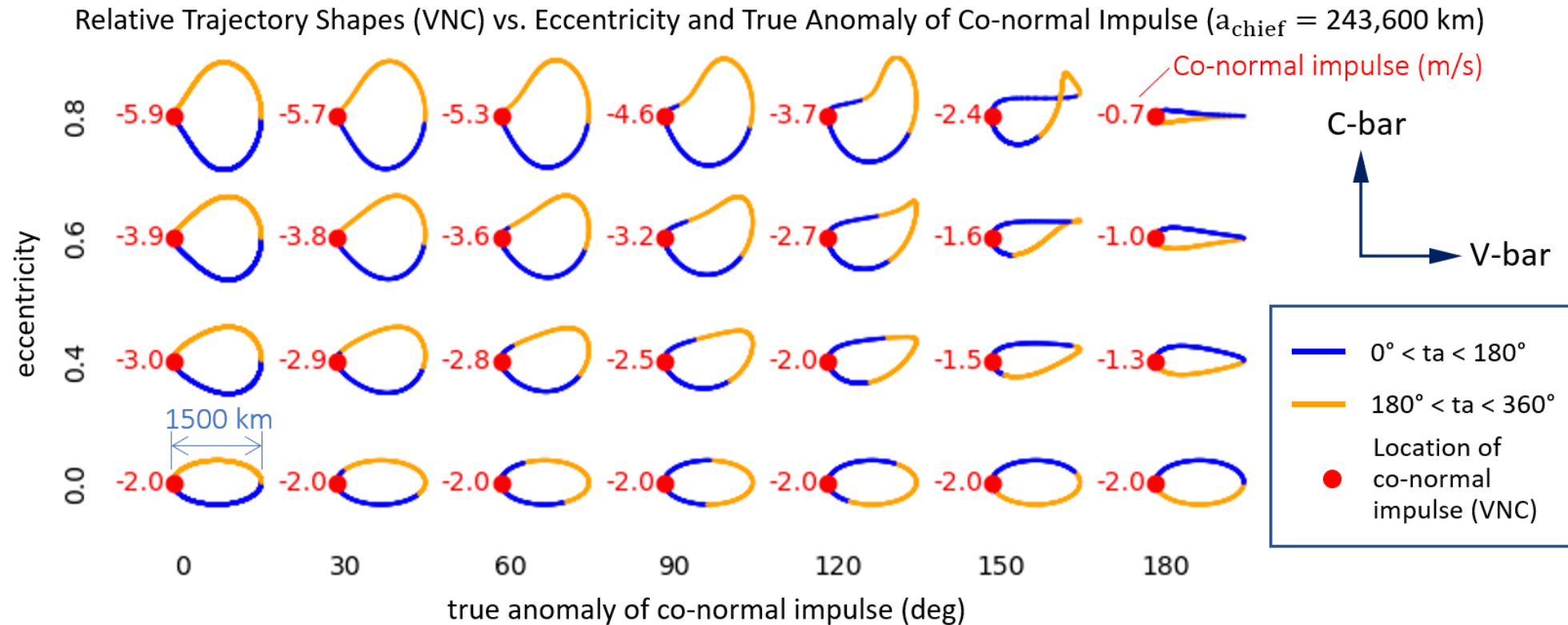
- Background
  - P/2 Lunar Resonant Orbits
  - Relative Motion in Eccentric Orbits
- Mission Design Method
- Insertion
- Maintenance
- Mission Design Applications
- Conclusion

# Background



Phasing loops leading to a P/2 LRO, in Earth Centered Inertial (ECI) and Earth-Moon rotating (ROT) frames. An eccentricity of approximately 0.65 places apogee near the Moon orbit radius and perigee above GEO (gold circle) and the outer Van Allen belt (green circle).

# Background

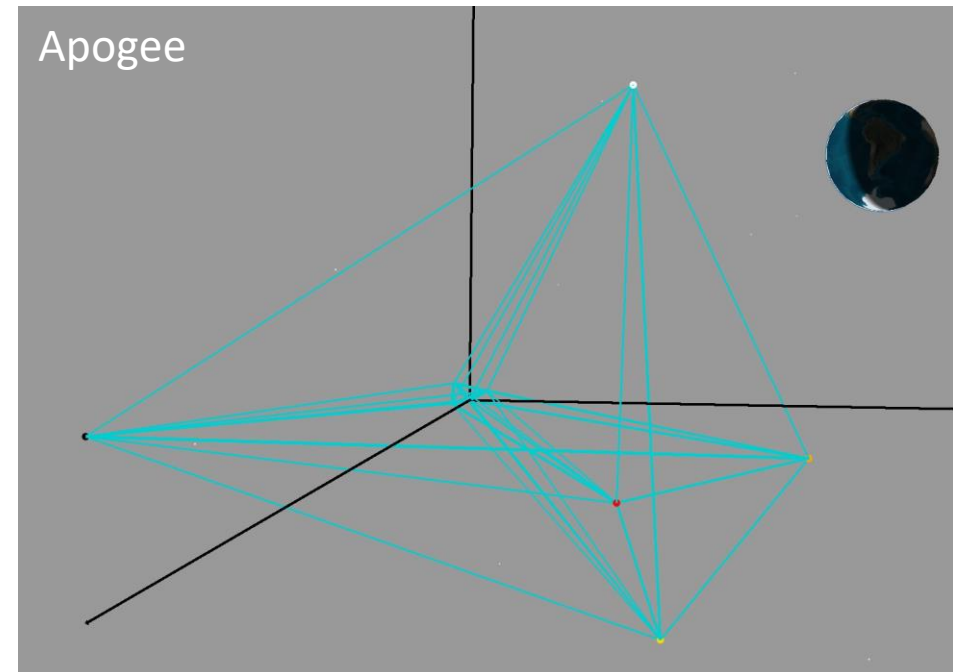
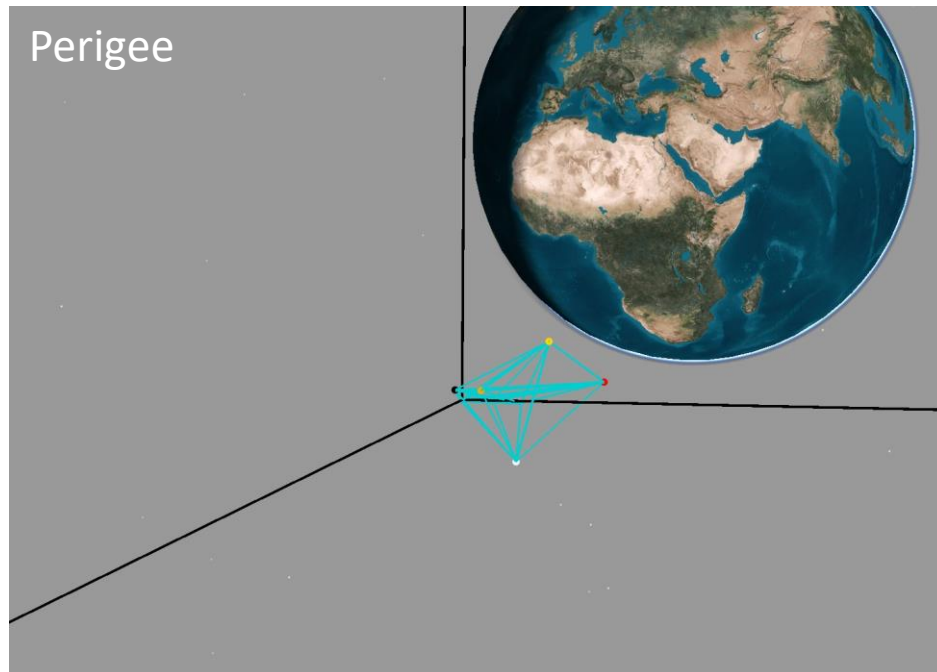


Relative trajectories in VNC coordinates, propagated using the Yamanaka-Ankersen STM. A co-normal impulse at the VNC origin induces the relative motion, and relative trajectories are shown as a function of the chief's eccentricity and the true anomaly of the co-normal impulse.

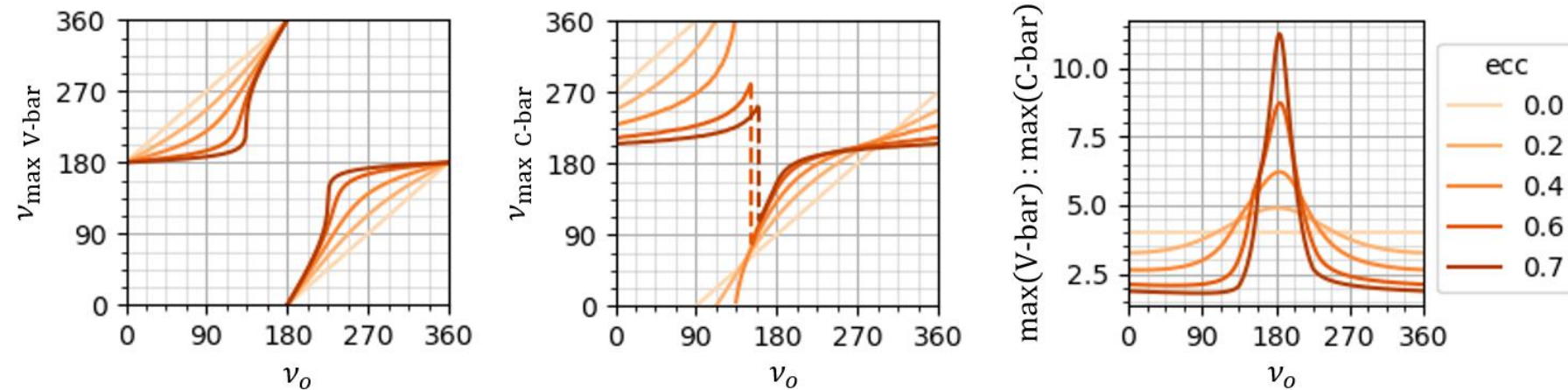
# Mission Design Method



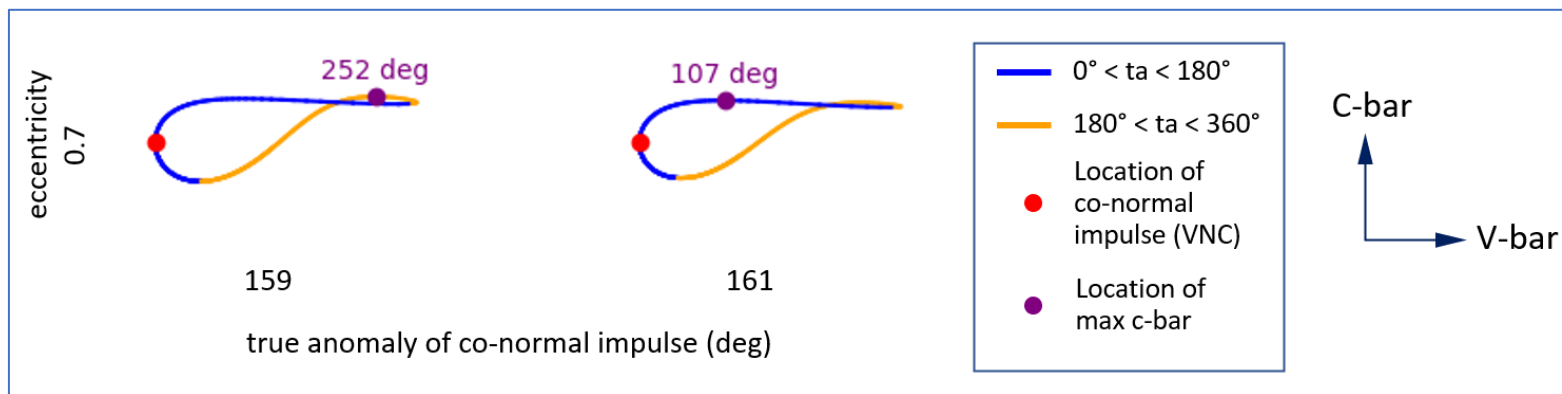
- Target VNC states at true anomaly ( $v$ ) values
- Deputies disperse near apogee to make observations
- The swarm contracts near perigee to allow crosslinks and downlink to ground
- Here we'll use 1500 km and 50 km as bounds on the swarm relative motion



# Insertion



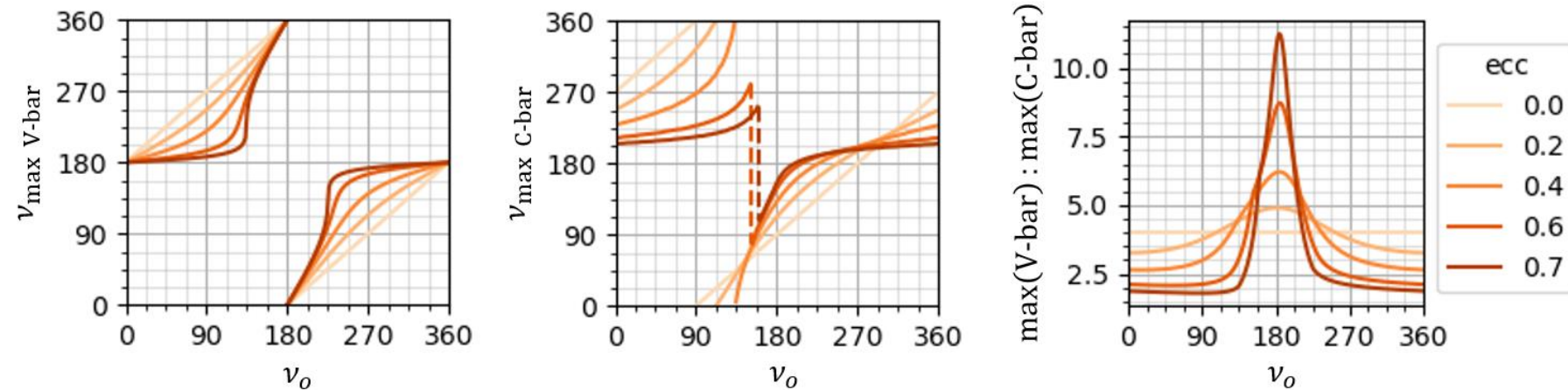
In-plane trends for a negative C-dot insertion at  $\nu_o$ .



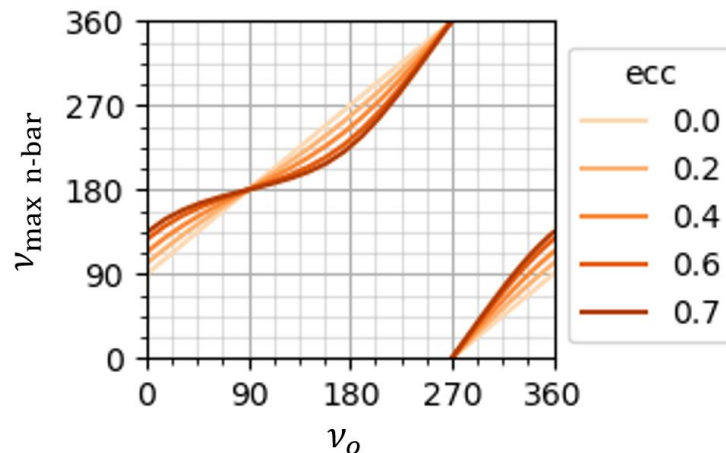
Example of a discontinuity in the location of maximum C-bar.

- The true anomaly of insertion ( $\nu_o$ ) affects relative trajectory shape in eccentric orbits
- In-plane motion is coupled, with maximum V-bar excursion typically larger than maximum C-bar excursion
- For moderate and high eccentricities, discontinuities occur in the location of the maximum c-bar excursion
- All examples shown use a negative C-dot insertion impulse

# Insertion



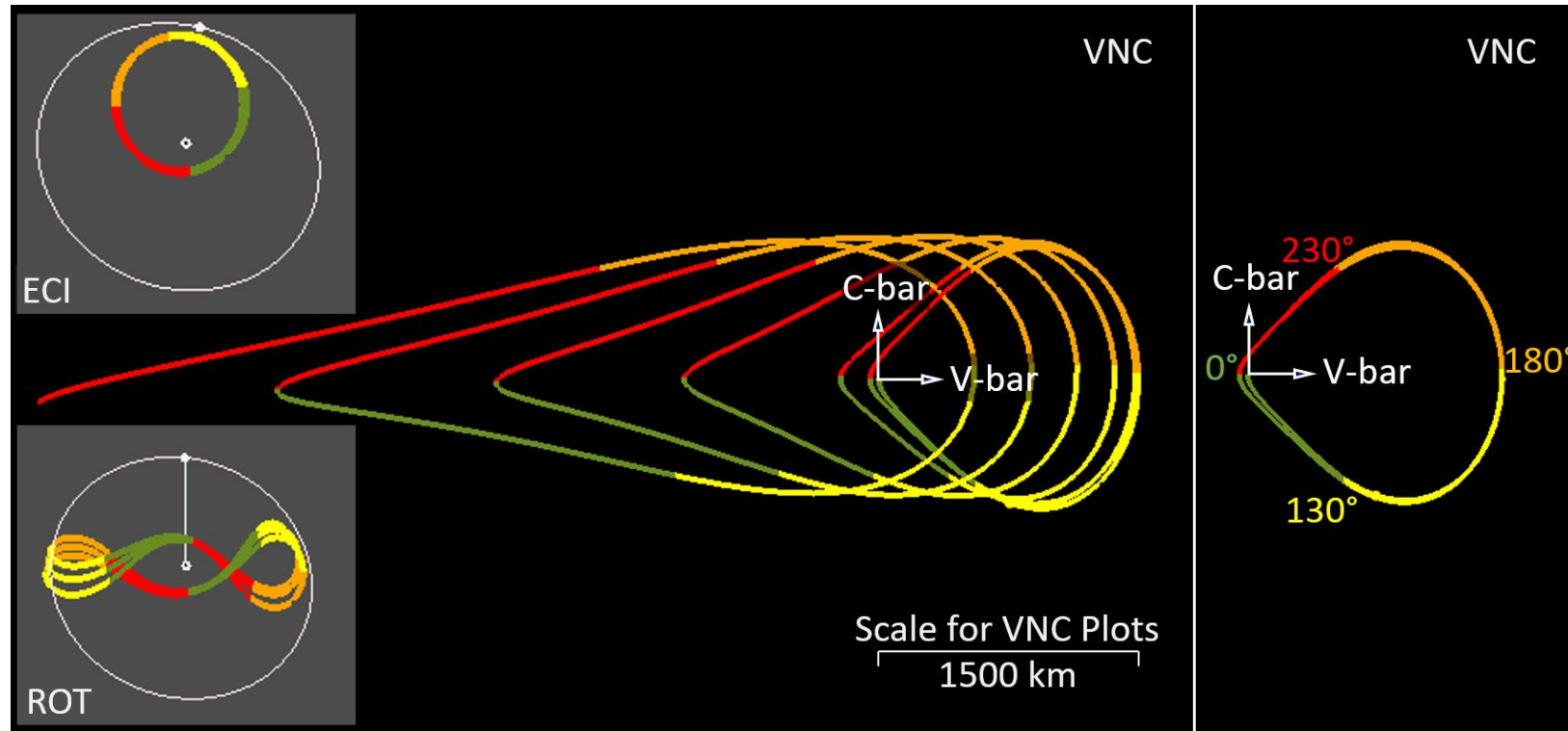
In-plane trends for a negative C-dot insertion at  $\nu_o$ .



Out-of-plane trends for a positive N-dot insertion at  $\nu_o$ .

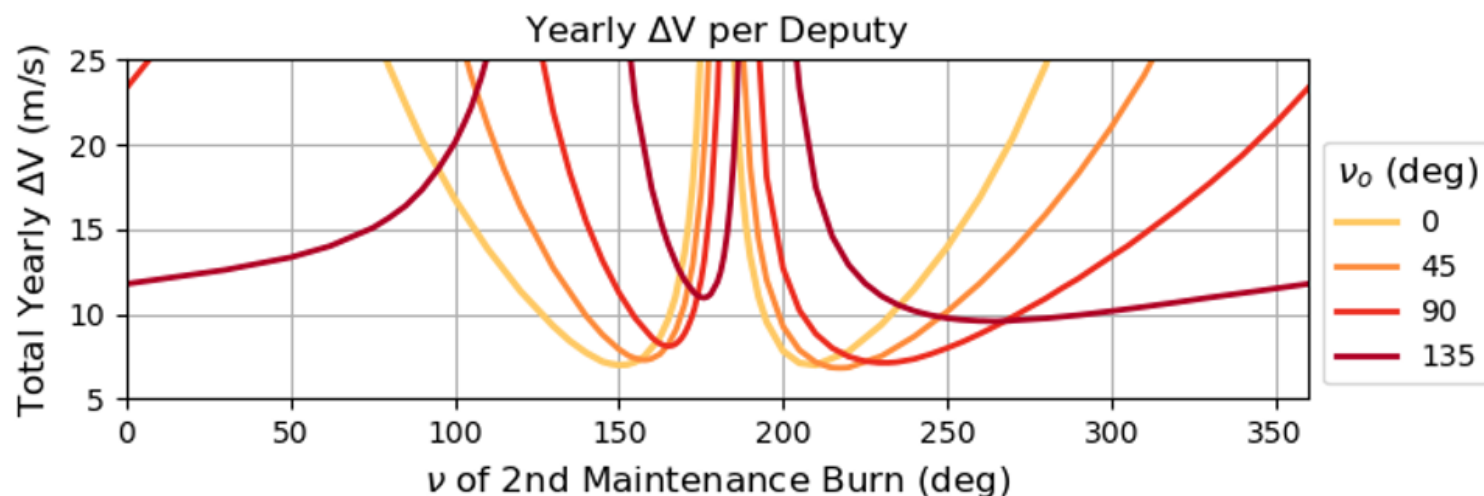
- Out-of-plane motion is decoupled from in plane motion
- For circular orbits, the maximum N-bar excursion occurs  $90^\circ$  from the N-dot insertion impulse
- For elliptical orbits, the maximum N-bar excursion tends to move closer to apogee

# Maintenance



Lunar-perturbed relative trajectory for uncontrolled (left) and controlled (right) example case, with six post-deployment revolutions shown. The controlled trajectory targets +1500 km V-bar at apogee and -50 km V-bar at perigee. Color arcs correspond to true anomalies between 0°, 130°, 180°, and 230°, as shown in the plot on the right. The insets on the left show the trajectory in ECI and ROT frames (at the scale of these insets, the chief-deputy system can be treated as a point mass). For this figure, forces included are lunar perturbations and  $J_2$  only.

# Maintenance

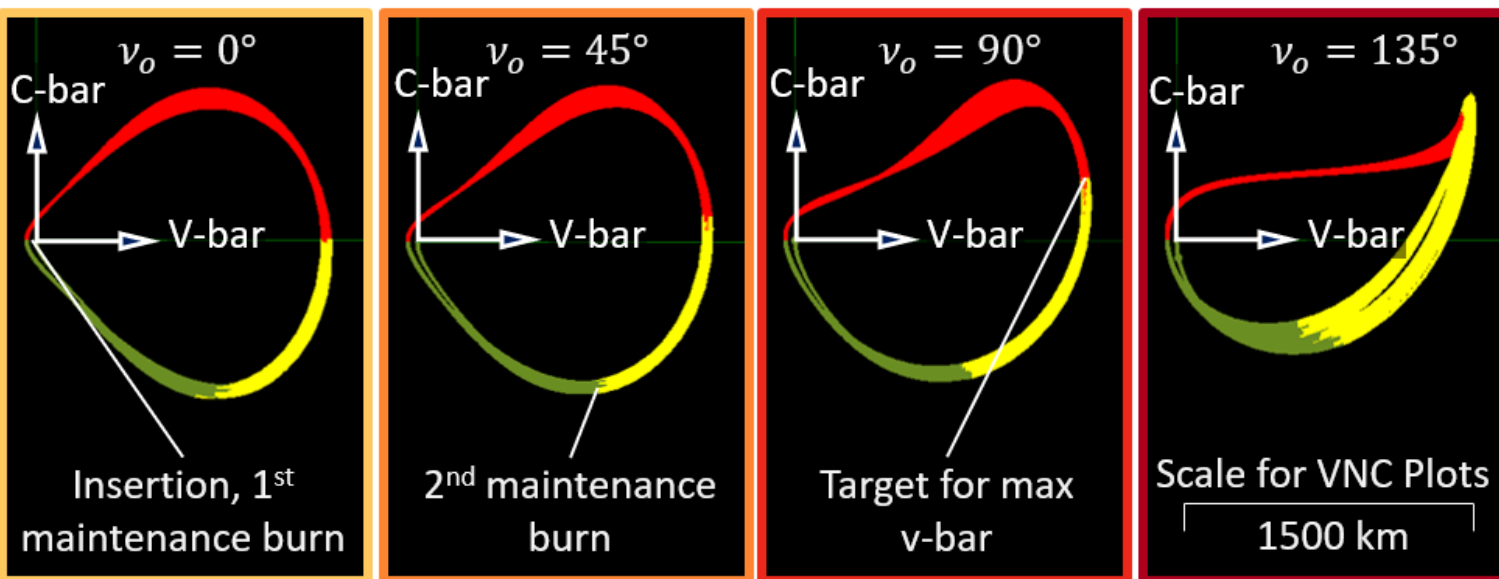


## In-Plane Maintenance

- A pair of maintenance burns, with the 1<sup>st</sup> at  $\nu_0$
- Varied  $\nu$  of 2<sup>nd</sup> burn and calculated yearly  $\Delta V$
- Repeated this process for a selection of  $\nu_0$  values to generate a family of delta-v curves

## Out-of-Plane Maintenance (not shown)

- Decoupled from in-plane maintenance
- N-bar excursion maintained using N-dot burns at relative line of nodes
- Position of relative line of nodes maintained with N-dot burns away from relative line of nodes

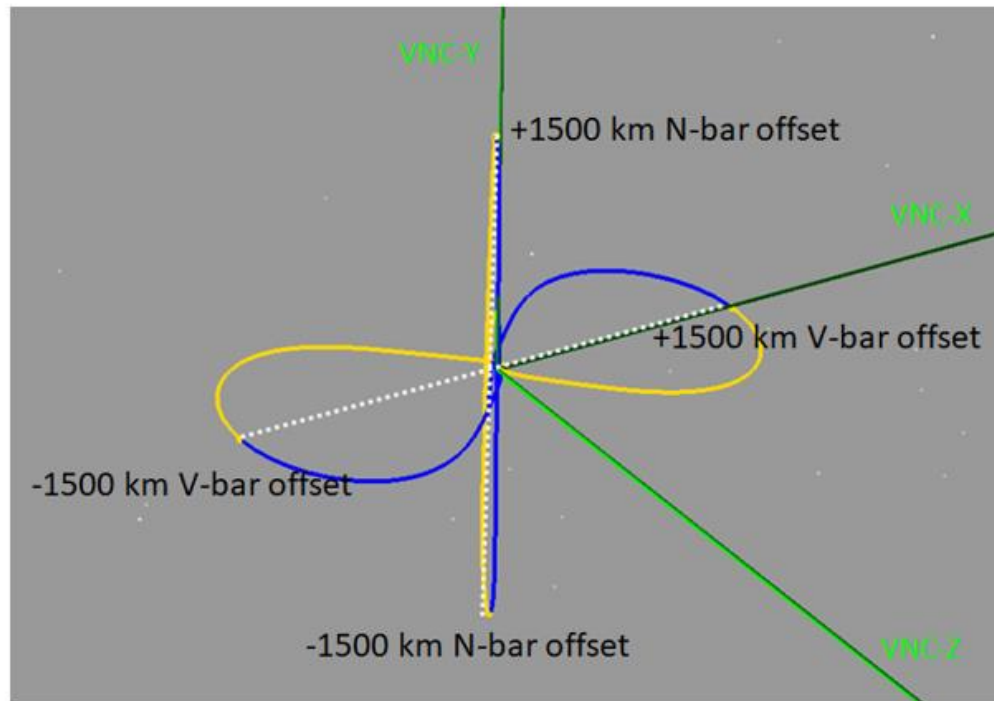


# Mission Design Applications

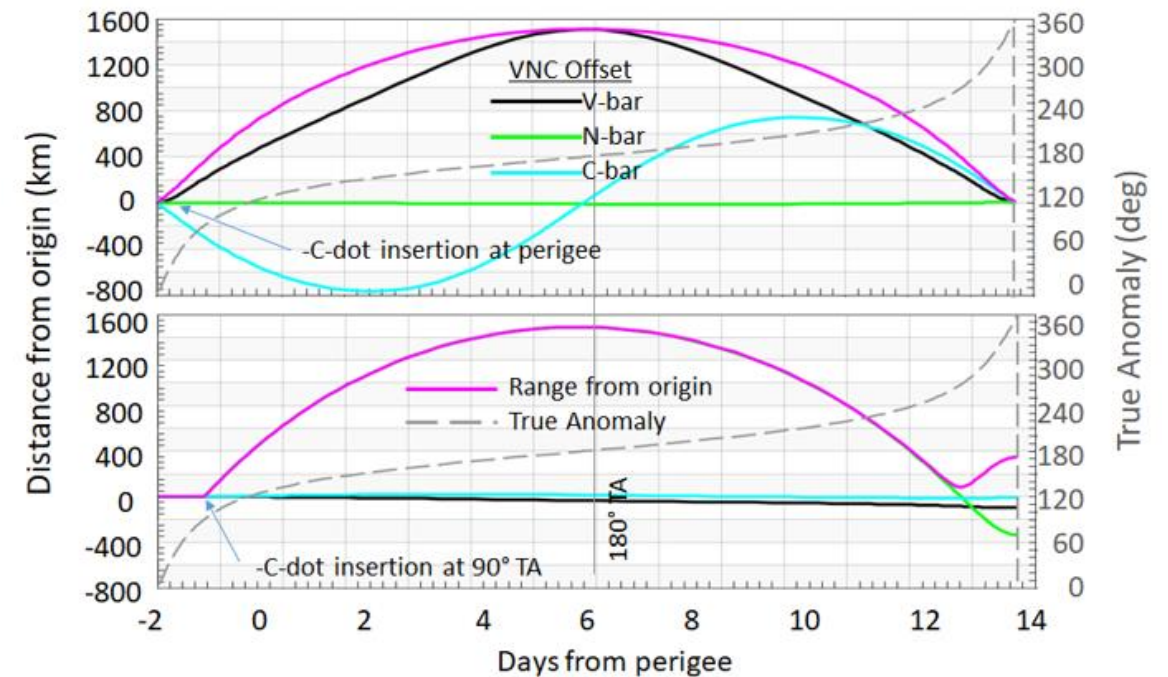


## Design Use Case #1: V-bar and N-bar separations

Orthogonal V-bar and N-bar offsets at apogee



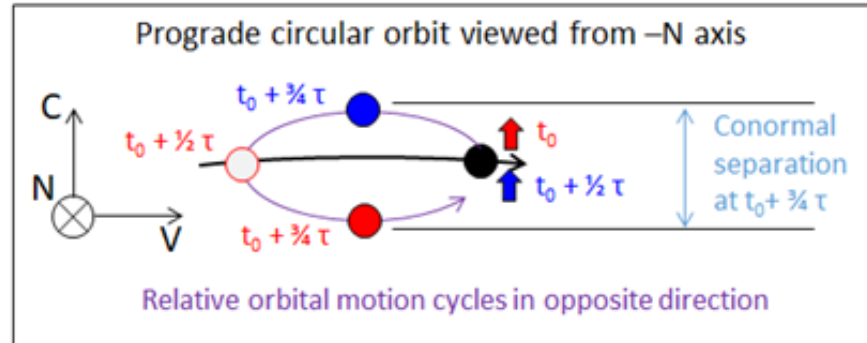
Separation components  
showing orthogonal V-bar and N-bar offsets at apogee



Design use case #1: examples of  $\sim 1500$  km maximum excursion at apogee in  $\pm V$  and  $\pm N$  directions. In-track offset for 242,000 km semimajor axis and 0.65 eccentricity orbit uses  $\pm 4.45$  m/s C-dot impulse at perigee. Out of plane offset of 1500 km uses  $\pm 6.5$  m/s N-dot impulse applied at  $\nu_0 = 90^\circ$ .

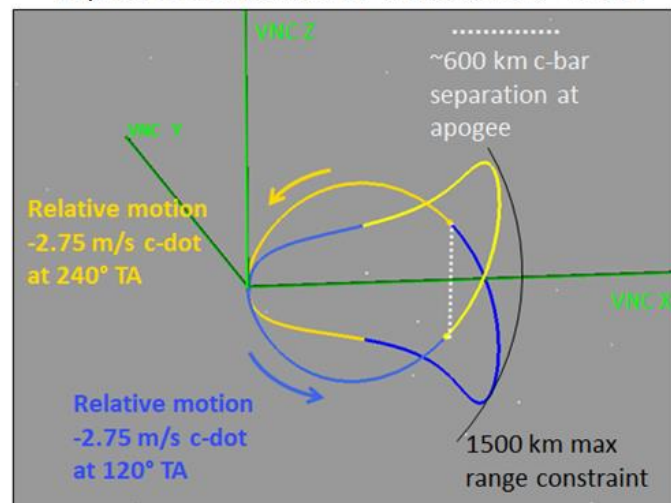
# Mission Design Applications

## Design Use Case #2: Addition of C-bar separations



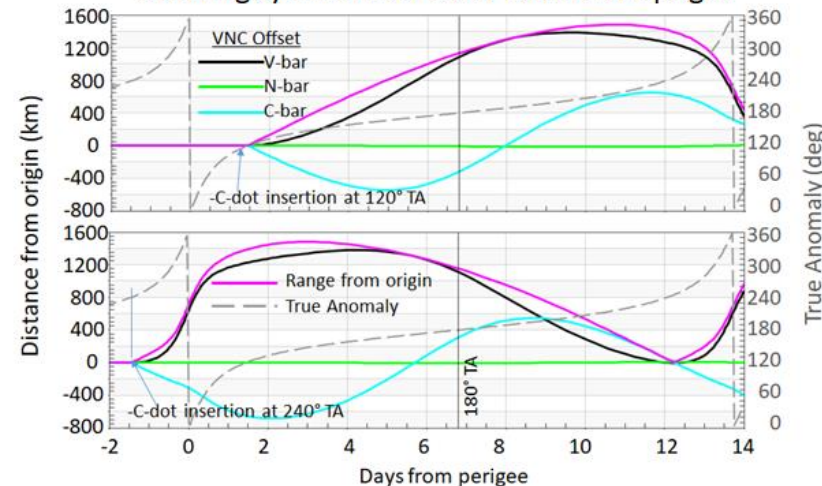
- In circular orbits, the use of multiple deputies with insertions separated by half the orbit period ( $\tau$ ) enables C-bar separations.
- In design use case #2 ( $a = 242,136$  km,  $e = 0.65$ ), insertions at  $v_o = 120^\circ$  and  $240^\circ$  result in symmetrical C-bar offsets at apogee.

In plane relative motion viewed from  $-N$  axis



Separation components

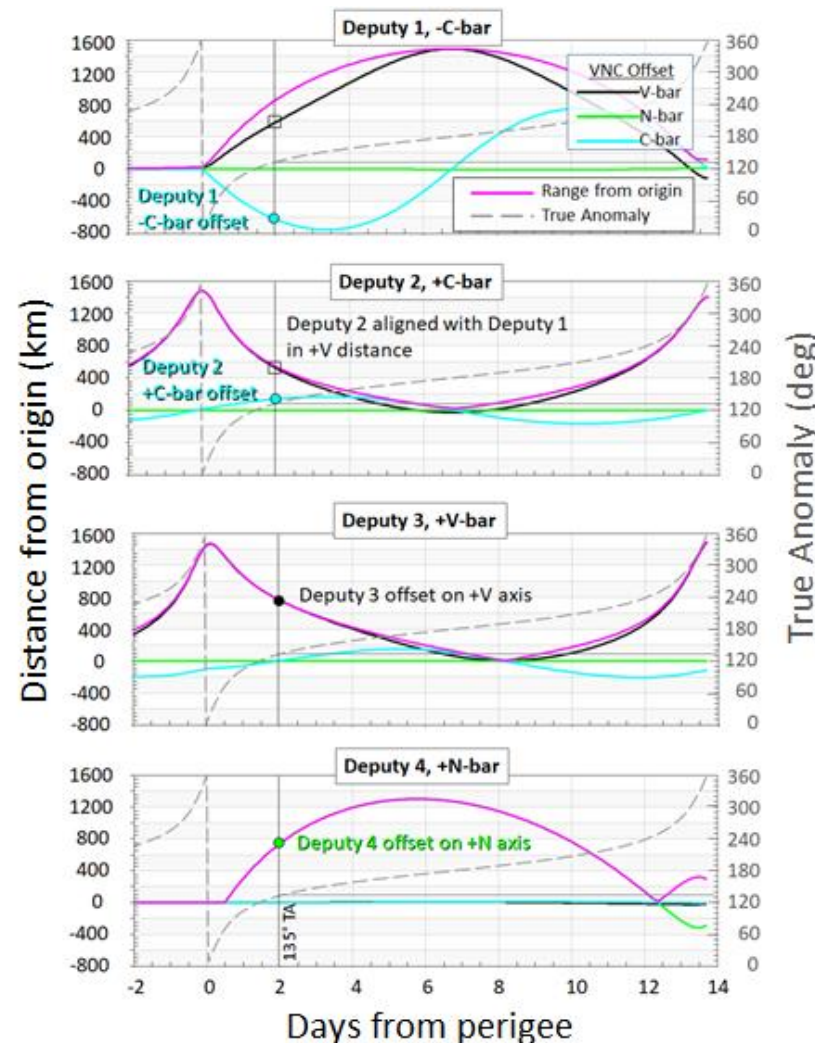
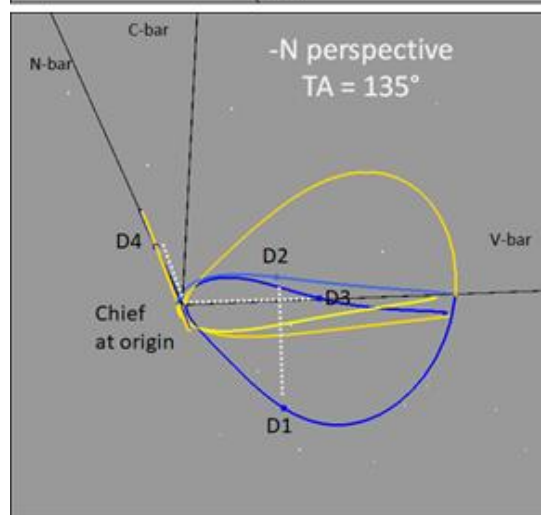
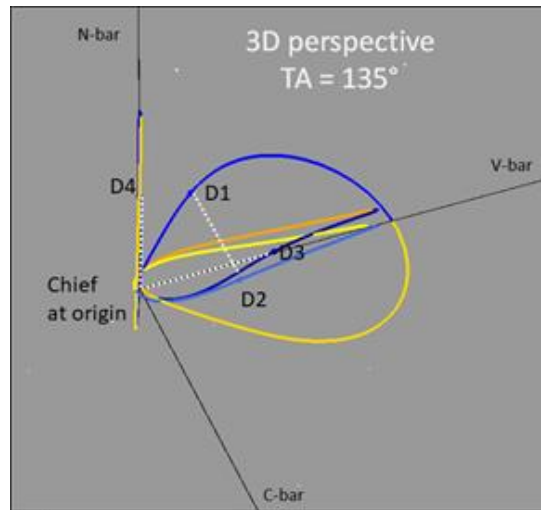
showing symmetrical C-bar offsets at apogee



Example	Relative motion target $v$ , (V, N, C) Deg, (km)	Insertion $v_o$ , $\Delta V$ , (V, N, C unit vector) Deg, m/s, (none)	Max range from Chief $v$ , Range, (V, N, C components) Deg, km, (km)
-C-bar	$180^\circ$ , (1100, 0, -300)	$120^\circ$ , 2.75, (0, 0, -1)	$215^\circ$ , 1500, (1350, 0, 600)
+C-bar	$180^\circ$ , (1100, 0, 300)	$240^\circ$ , 2.75, (0, 0, -1)	$145^\circ$ , 1500, (1350, 0, -600)
+V-bar	$180^\circ$ , (600, 0, 0)	$0^\circ$ , 1.6, (0, 0, -1)	$180^\circ$ , 600, (600, 0, 0)
+N-bar	$180^\circ$ , (0, 600, 0)	$90^\circ$ , 2.7, (0, 1, 0)	$180^\circ$ , 600, (0, 600, 0)

# Mission Design Applications

## Design Use Case #3: Larger C-bar offsets with asymmetrical insertions

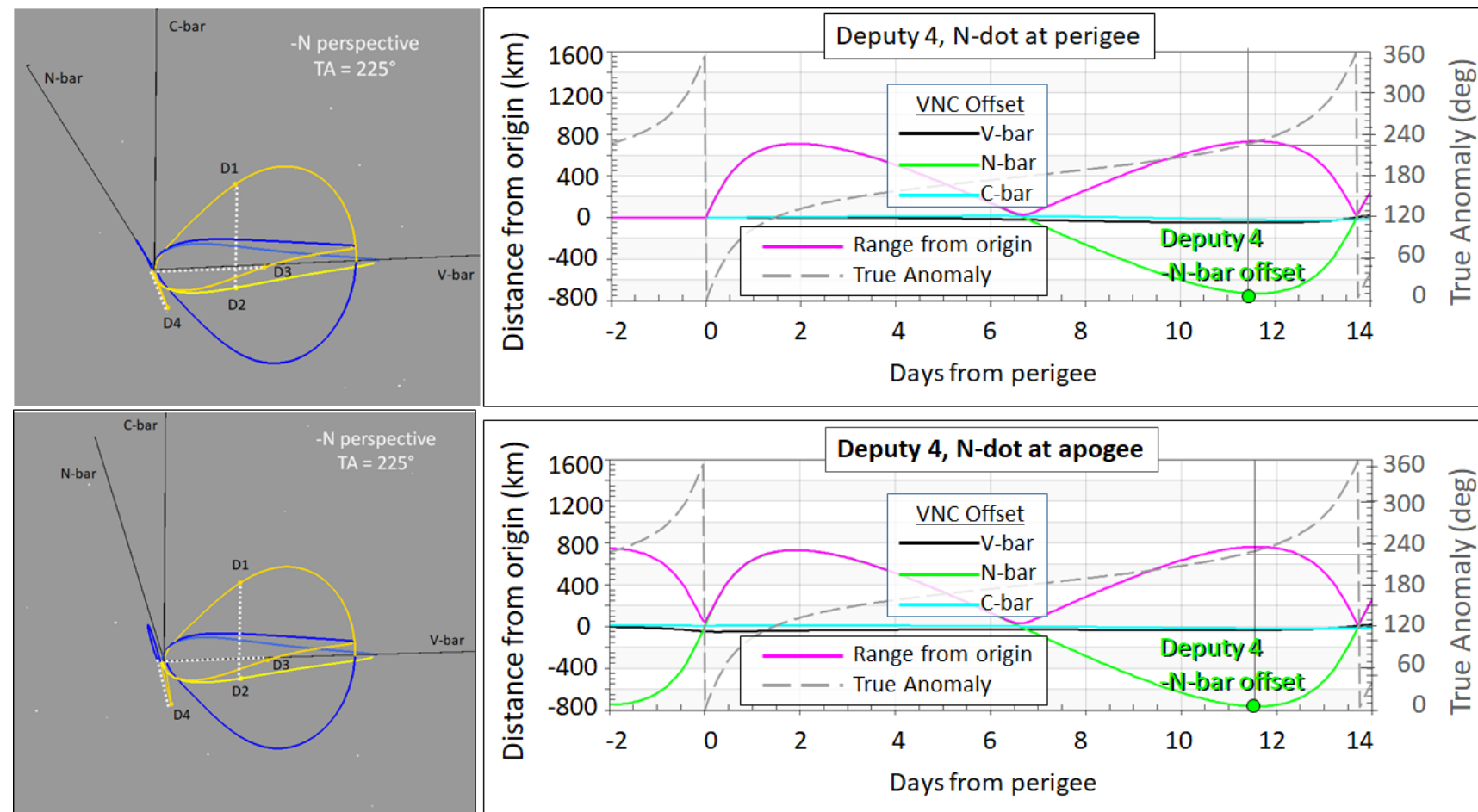


- Asymmetrical insertions enable larger C-bar offsets than in Design Use Case #2
- Design Use Case #3 uses insertions at apogee and perigee to create 750 km C-bar separations at  $\nu = 135^\circ$
- The configuration evolves more quickly than Design Case #2's symmetrical configuration

Deputy	Relative motion target $\nu$ , (V, N, C) Deg, km	Insertion $\nu_0$ , $\Delta V$ , (V, N, C unit vector) Deg, m/s, none
1	135°, (550, 0, -600)	0°, 4.45, (0, 0, -1)
2	135°, (550, 0, 150)	180°, 0.88, (0, 0, -1)
3	135°, (750, 0, 0)	190°, 0.95, (0, 0, -1)
4	135°, (0, 750, 0)	70°, 7.25, (0, 1, 0)

# Mission Design Applications

## Design Use Case #4: Symmetrical offsets at $\nu \approx 135^\circ$ and $\nu \approx 225^\circ$



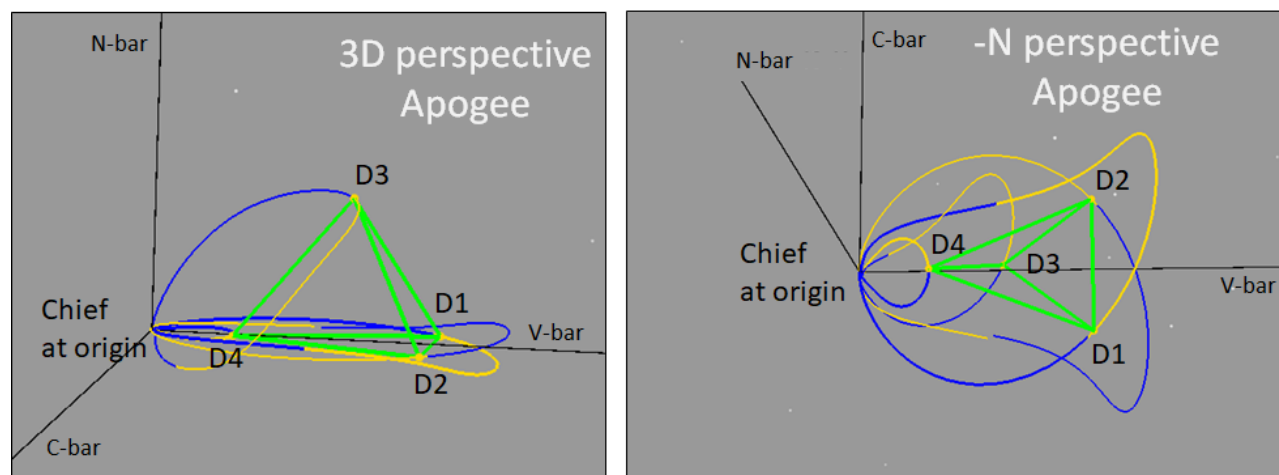
- N-dot insertions at perigee or apogee enable symmetrical N-bar offsets twice per rev
- In Design Use Case #4, equal and opposite offsets occur at  $\nu \approx 135^\circ$  and  $\nu \approx 225^\circ$

Deputy	Relative motion target $\nu$ , (V, N, C) Deg, km	Insertion $\nu_o$ , $\Delta V$ , (V, N, C unit vector) Deg, m/s, none
1	225, (550, 0, 600)	0, 4.2, (0, 0, -1)
2	225, (550, 0, -150)	180, 0.88, (0, 0, -1)
3	225, (750, 0, 0)	170, 0.95, (0, 0, -1)
4 (Two options)	225, (0, 750, 0) 225, (0, 750, 0)	0, 11.5, (0, 1, 0) 180, 2.4, (0, -1, 0)

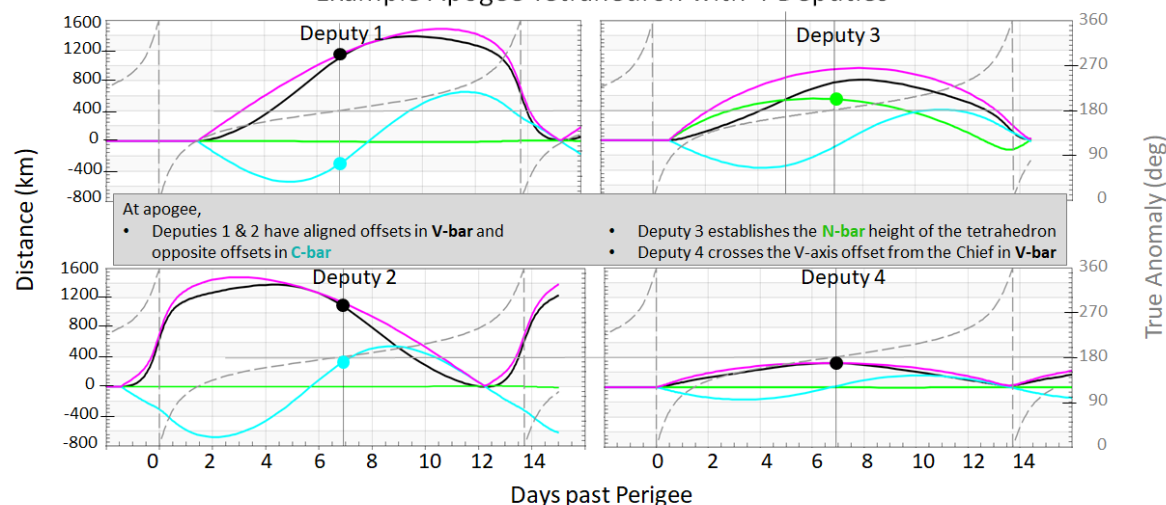
# Mission Design Applications

## Design Use Case #5: Near-regular tetrahedron at apogee

- Tetrahedra provide a useful geometry for many multi-satellite swarms
- Design Use Case #5 has the goal of creating the largest near-regular tetrahedron possible while meeting the 1500-km max distance constraint
- The deputies form a near-regular tetrahedron at apogee; away from apogee, the tetrahedron loses its near-regular geometry



Example Apogee Tetrahedron with 4 Deputies

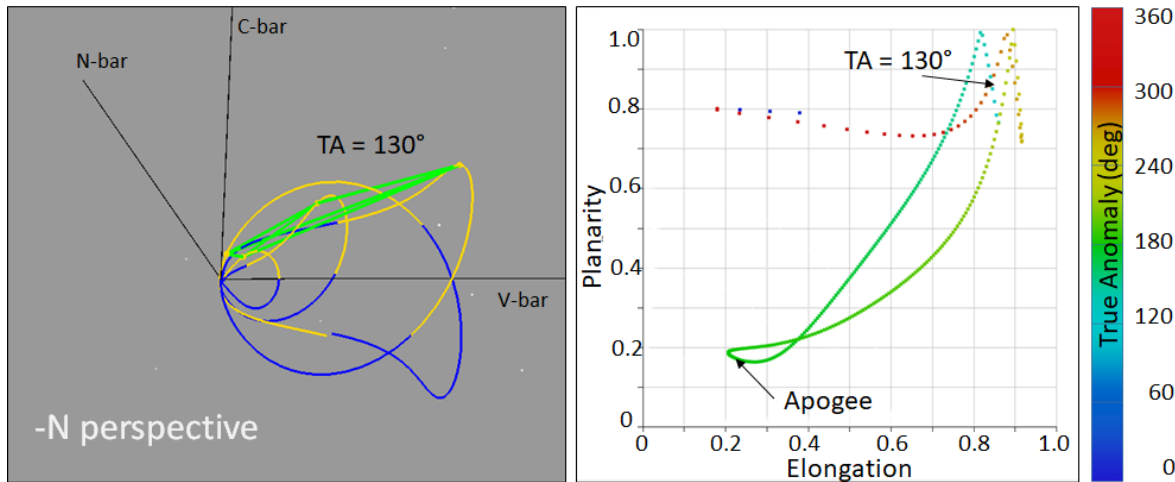


Deputy	Relative motion target $v$ , (V, N, C) Deg, km	Insertion $v_o$ , $\Delta V$ , (V, N, C unit vector) Deg, m/s, none
1	180°, (1000, 0, -325)	120°, 2.7, (0, 0, -1)
2	180°, (1000, 0, 325)	240°, 2.7, (0, 0, 1)
3	180°, (750, 550, 0)	80°, 3.4, (0, 0.81, -0.59)
4	180°, (325, 0, 0)	0°, 1, (0, 0, -1)

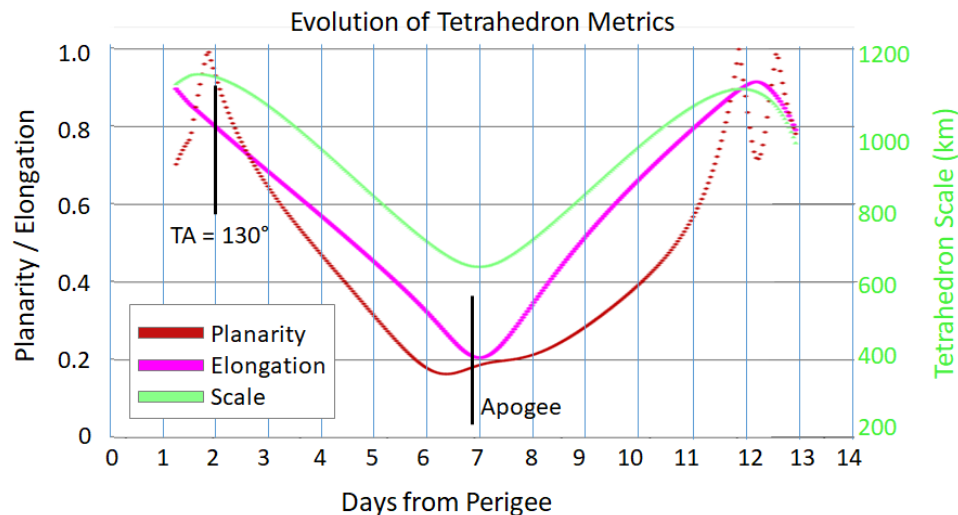
# Mission Design Applications



## Design Use Case #5: Near-regular tetrahedron at apogee

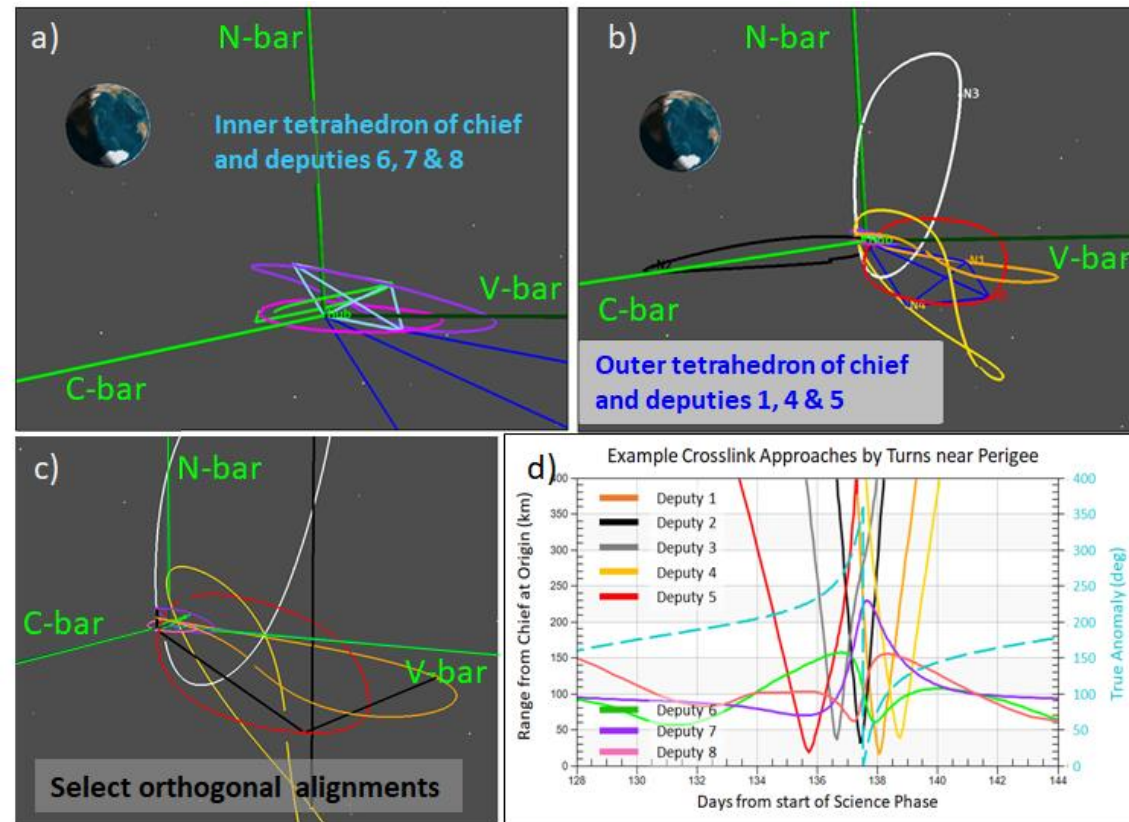


- Tetrahedra provide a useful geometry for many multi-satellite swarms
- Design Use Case #5 has the goal of creating the largest near-regular tetrahedron possible while meeting the 1500-km max distance constraint
- The deputies form a near-regular tetrahedron at apogee; away from apogee, the tetrahedron loses its near-regular geometry



Note: see *Analysis Methods for Multi-Spacecraft Data*, ch. 13 for a discussion of planarity, elongation, and scale

# HelioSwarm



- The HelioSwarm mission concept provides an example application of multi-satellite swarm design in P/2 LRO
- HelioSwarm uses multiple deputies to form tetrahedra and orthogonal offsets near apogee, contracting near perigee to enable data crosslink and downlink via the chief

Chief or Deputy number	Relative motion target $v$ , (V, N, C) Deg, km	Additional placement $v$ , (V, N, C) Deg, km	Insertion $v_o$ , $\Delta V$ , (V, N, C unit vector) Deg, m/s, none
Chief	0 - 360°, (0, 0, 0)	0 - 360°, (0, 0, 0)	N/A
1	180°, (1275, -180, -225)	155°, (625, -150, -600)	90°, 4.1, (0, -0.24, -0.97)
2	180°, (-1525, -175, -75)	No secondary target	280°, 3.3, (0, 0.21, 0.98)
3	180°, (600, 1200, 100)	No major secondary function	90°/270°, 6.5, (0, $\pm 0.98$ , -0.2)
4	180°, (750, -900, -250)	155°, (150, -550, -275)	120°/300°, 3.9, (0, $\pm 0.75$ , -0.65)
5	135°, (800, -325, -300)	155°, (825, -400, -250)	240°, 3.3, (0, 0.62, 0.78)
6	155°, (90, 40, -40)	180°, (0, 20, 50)	240°, 0.9, (0, 1, 0) 270°, (0, 0, -1)
7	135°, (110, 60, 10)	180°, (-100, 50, 20)	200°, 0.3, (0, 0.559, -0.825)
8	135°, (110, -20, 10)	180°, (0, -10, 60)	225°, 0.4, (0, -0.87, -0.49)

HelioSwarm reference mission swarm design, illustrating the formation of multiscale tetrahedra, orthogonal alignments, and crosslink approaches that recur in every cycle of true anomaly.

# Conclusion



- VNC targeting provides a convenient framework for relative motion design in eccentric P/2 LRO
- Relative orbits in P/2 LRO require maintenance due to significant gravitational perturbations
- Expansion of swarms near apogee allows for extended periods of science data collection, and contraction near perigee allows for data crosslink and downlink
- $\Delta V$  budget is reasonable – as low as 7 m/s/yr per deputy for  $\nu_o$  near perigee
- Selection of VNC targets enables multi-satellite missions to form recurring 3-dimensional geometries to meet mission goals

# Selected References



(Full reference list in conference proceedings)

- Plice, L., A. Dono-Perez, and S. West 2019. "HelioSwarm: Swarm Mission Design in High Altitude Orbit for Heliophysics". AAS 19-831.
- Yamanaka, K., F. Ankersen 2002. "New State Transition Matrix for Relative Motion on an Arbitrary Elliptical Orbit". Journal of Guidance, Control and Dynamics, Vol. 25, No. 1.
- Paschmann, G. and P. Daly (eds.). *Analysis Methods for Multi-Spacecraft Data*, Ch. 13, ISSI Scientific Reports Series, ESA/ISSI, Vol. 1. ISBN 1608-280X, 1998.